

# Hydroxyapatite/High-Performance Polyethylene Fiber Composites for High-Load-Bearing Bone Replacement Materials

N. H. LADIZESKY,<sup>1</sup> I. M. WARD,<sup>1</sup> W. BONFIELD<sup>2</sup>

<sup>1</sup> IRC in Polymer Science and Technology, University of Leeds, Leeds LS2 9JT, United Kingdom

<sup>2</sup> IRC in Biomedical Materials, Queen Mary and Westfield College, University of London, London E1 4NS, United Kingdom

Received 5 December 1996; accepted 15 January 1997

**ABSTRACT:** A combination of three technologies, high-performance fiber processing, fiber compaction, and hydrostatic extrusion has been used to produce hydroxyapatite/polyethylene bone analog composites with the highest stiffness and strength yet encountered in these systems, fully matching the values associated with cortical bone. These advantages of the new materials are complemented by satisfactory ductility. Observation of the melting behavior of the composites, together with an analysis of their hydrostatic extrusion characteristics, provides some understanding of the mechanisms leading to their superior mechanical performance. © 1997 John Wiley & Sons, Inc. *J Appl Polym Sci* **65**: 1865–1882, 1997

**Key words:** artificial bone; hydroxyapatite; high modulus polyethylene fibers; hydrostatic extrusion; mechanical properties

## INTRODUCTION

It has long been recognized that molecular orientation in a polymer leads to a significant enhancement in the stiffness and strength along the orientation direction, as well as providing a means of tailoring the material anisotropy.<sup>1</sup> These effects are enhanced in high-density polyethylene because of its simple molecular structure.<sup>2</sup> There are several well-established technologies for inducing molecular orientation in polymeric materials, namely tensile drawing,<sup>3–6</sup> die drawing,<sup>7</sup> and hydrostatic extrusion.<sup>8–12</sup> A combination of these technologies may be used for particular applications, while composites with a polymeric matrix could also benefit from the molecular orientation approach.

Melt-spun linear polyethylene fibers may be drawn at temperatures below their melting point to produce a high degree of molecular orientation.<sup>3,13</sup> This material, known as high modulus polyethylene (HMPE) fibers, exhibits enhanced stiffness and strength. Draw ratios (DR, ratio of the initial and final cross-sectional areas) over 30 : 1 have been achieved, in which cases the axial modulus and strength of the fibers are ~ 40 and 1.3 GPa, respectively. To place these values in perspective, spun polyethylene fibers have a modulus < 1 GPa while its strength is of the order of 100 MPa.

Hot compaction of an array of melt-spun HMPE fibers has recently been developed and allows the production of large-section polymeric products with substantial fiber morphology content, retaining to a large extent the high stiffness and strength associated with the fibers.<sup>14–16</sup> It was found<sup>14</sup> that only ~ 10% of the fiber has to melt in order to fill all the voids and bind the fibers

---

Correspondence to: I. M. Ward.

© 1997 John Wiley & Sons, Inc. CCC 0021-8995/97/101865-18

together, forming a solid structure. This is achieved at an optimal temperature which has to be controlled within 0.5°C, a technically acceptable limit even for products of relatively large geometrical dimensions. Increasing the compaction temperature from the optimal value gives rise to further melting and accompanying reduction of the fiber morphology phase, leading to lower mechanical properties.

The growing understanding of the complex interactions between implants and natural tissue has led to the development of a new type of composite material, namely polyethylene (PE) reinforced with synthetic hydroxyapatite (HA).<sup>17-20</sup> This system represents an attempt to mimic the two main levels of mechanical behavior of bone, a compliant matrix (collagen) reinforced with a brittle ceramic (hydroxyapatite). It was shown that 40 vol % HA can be incorporated into the PE with a hot compounding process. This amount of reinforcement produces a bone substitute with the ceramic particles homogeneously distributed in the polymeric matrix, ductility within the bounds of cortical bone, stiffness and strength suitable for prostheses under minor physiological loads, fracture toughness superior to bone, and favorable bioactivity such as to encourage bone apposition, resulting in the virtual disappearance of the boundary between the natural bone and the composite a few months after implantation.<sup>21-24</sup> This material has now been commercialized under the name of HAPEX<sup>TM</sup> (Smith and Nephew, Richards, Memphis, TN, USA) and it has found use in a range of minor load-bearing applications, including orbital floor reconstruction<sup>25</sup> and otologic implants. However, it does not have the stiffness and strength to be used in major load-bearing applications, such as total hip joint replacement.

A previous communication<sup>26</sup> has reported the successful hydrostatic extrusion of HAPEX<sup>TM</sup> to produce an oriented matrix. The process involved a billet of the composite surrounded by a fluid and heated up below its melting point. The billet is made to pass through a convergent die by the application of a back pressure to the fluid. The extrusion ratio (ER) is defined as the ratio of the cross-sectional area of the billet to that of the die bore. It was found that extrusion of HAPEX<sup>TM</sup> composite to an extrusion ratio of 8 : 1 increased its flexural stiffness and strength by > 100%, reaching values within the lower the range of cortical bone. It is of interest to note that these improvements were not achieved at the expense of reduced ductility,

rather, a 400% increase of the strain to failure was also found.

However, alternative routes may enable the production of materials with increased HA content (for higher bioactivity) and better mechanical properties, particularly stiffness. Thus the basic concept of combining PE with HA to produce bone analog materials could also be fulfilled by replacing the isotropic polymer with chopped HMPE fibers,<sup>2,3,5</sup> followed by hot compaction.<sup>14</sup> This article describes such an approach. The material was amenable to hydrostatic extrusion, a technology never previously attempted with hot compacted fibers. The composites were evaluated in terms of their flexural stiffness, strength, and ductility. A qualitative assessment of the effect of the various processing stages on the matrix morphology was made with differential scanning calorimetry (DSC). The dispersion of the phases in the HA/PE composites was studied with optical microscopy.

## EXPERIMENTAL

### Materials

Hydroxyapatite is a calcium phosphate ceramic [ $\text{Ca}_{10}(\text{PO})_6(\text{OH})_2$ ]. Grade P88, a synthetic hydroxyapatite was used, with 4.14- $\mu\text{m}$  average particle size<sup>24</sup> and a density of 3.156 g cm<sup>-3</sup> (Biotol Ltd, UK). Chopped HMPE fibers were supplied by Hoechst Celanese Fibers (Charlotte NC, USA), from continuous fibers manufactured by SNIA Fibers (Cesano Maderno, Italy). Some samples also contained a third type of material, namely 40 vol % HA/60 vol % PE (HAPEX<sup>TM</sup>).<sup>25</sup> The polymer for this material was Rigidex HM 4560PX (BP Chemicals Ltd., UK) while the HA was again P88 grade.

Table I gives the main parameters of the PE and HA used in this work.

### Preparation of Composites

The HA particles and chopped fibers were mixed at room temperature with a Braun Hand Blender MR 350 and the HC chopper accessory [Braun (UK) Ltd., London]. This equipment was found particularly convenient because the hand-held motor casing and the chopper are both axially aligned, allowing the blending to be carried out at an inclined angle while rolling the lower end on the bench. This procedure assisted the move-

**Table I Material Characterization**

Material	Value
HA (P88)	
Density	3.156 g/cm <sup>3</sup>
Particle size	4.14 <sup>a</sup> μm
HMPE fiber	
Density	0.960 g/cm <sup>3</sup>
$\bar{M}_w$	130,000
$\bar{M}_n$	12,000
DR	30 : 1
Diameter	13 μm
Tensile modulus	40 GPa
Tensile strength	1.3 GPa
Fracture strain	5%
Segment length of chopped fiber	3.5 mm (SD = 0.3)
Rigidex HM 4560XP	
Density	0.945 g/cm <sup>3</sup>
$\bar{M}_w$	225,000
$\bar{M}_n$	24,000
Tensile modulus	0.68 GPa
Tensile strength	23.5 MPa
Fracture strain	>300%

<sup>a</sup> From ref. 24.

ment of the fibers inside the container and avoided agglomeration. The chopper accessory was modified to improve efficiency, namely, (1) a second pair of blades was added midway along the shaft, (2) the nylon bearings were replaced by stainless steel ball bearings, and (3) the plastic base was replaced by a heavier aluminum base. Mixing of 5 g of chopped fibers plus the required amount of HA was carried out for ~ 3 min using the three available motor speeds and rest periods in a reproducible sequence. This technique will be referred to as "room temperature" blending.

A small number of samples with 30 vol % HA (as supplied) were prepared using HA particles and HMPE chopped fibers mixed with an alternative technique. This is referred to as "liquid nitrogen" blending and it was developed at a later stage in connection with other experiments. Briefly, the technique involved the dispersion of the HA particles in liquid nitrogen followed by immersion of the chopped fibers, ensuring a continuous and gently boiling action of the liquid. When evaporation was completed, the HA particles remained fully incorporated into the network of fibers. On the other hand, room temperature blending involved some wastage of HA because particles escaped as dust and, in addition, a small

amount of powder was left unmixed in the container. This wastage was qualitatively taken into account by starting the mixing with a small excess of HA.

The composites were compacted in an aluminum mold placed in a hydraulic hot press. The samples were 150- × 10-mm rectangular bars, while the thickness varied between 2 and 8 mm, according to the sample use. The temperature during compaction was monitored with a probe connected to an electronic thermometer, inserted as a tight fit into holes bored at various points on the mold. The space between the hot plates of the press was shielded with Perspex sheets. Thus a predetermined molding temperature (usually ~ 136.0°C) in the middle of the mold could be achieved within 0.3°C, while the gradient between the two ends of the mold was 0.5°C.

The blended material inside the mold was maintained at the predetermined temperature for 20 min under low pressure to ensure good thermal contact between the mold and the two hot plates of the press. The compression load was then increased rapidly to 9 tonne (60 MPa pressure), when the heating was switched off and water cooling of the hot press started. The mold was maintained at constant pressure until it reached a temperature of 50°C, ~ 30 min, after which it was left on a bench to cool to room temperature before removing the sample.

Some samples were powderized to improve the HA distribution within the polymeric matrix. The powderizing process included three stages; (1) crushing in a fly press, (2) chopping with a Kenwood Chef Food Mixer fitted with the spice mill attachment (Kenwood Ltd., Hampshire, UK), and (3) powderizing in a Fritsch Pulverisette 14 Rotor-Speed Mill (Fritsch GmbH, Idai-Oberstein, Germany) using progressively finer perforation sieves, namely 6 mm, 2 mm, 1 mm, 500 μm, and, when required, 200 μm and 80 μm. The Rotor-Speed Mill was fitted with a 12-knife stainless steel rotor and the speed used was 16,000 r.p.m.

Powderizing could be readily achieved down to a 1-mm perforation sieve. Finer sieves required considerable care owing to heat generation, which could lead to melting of the polymer. The material to be fed into the Rotor-Speed Mill was kept in a beaker immersed in liquid nitrogen; however, no liquid nitrogen was poured into the machine.

After powderizing, the material was recomacted. At this stage it was necessary to remelt the PE fraction which melted during the first compaction, while producing minimum disturbance of

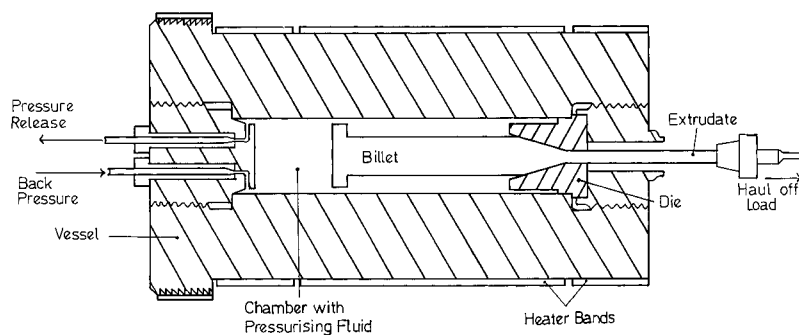


**Figure 1** Schematic diagram of the hydrostatic extrusion rig.

the nonmelted fraction. This was achieved by recompacting at 3–4°C lower than the temperature used during the first compaction (the HMPE fibers melt at ~ 140°C, which compares with ~ 130°C for recrystallized PE).<sup>14</sup>

Some composites were prepared in a somewhat different way, namely the chopped HMPE fibers were blended with a mixture of HA and HAPEX™ composite (40 vol % HA). The latter was prepared as described previously<sup>25</sup> and was available in coarse powder form. The HA and HAPEX™ composite were blended in a Waring 8011G Rotary Blender fitted with the stainless steel minicontainer type MC3 (Waring Products Div., Dynamics Corporation of America, Connecticut 06057, USA). The mixing was carried out using a reproducible sequence of blending pulses (15 s), tapping and scraping the container with a metal spatula. The powder obtained was molded in a stainless steel mold placed in a hydraulic press at 180°C under a 60-MPa load. The samples were cylindrical rods 60 mm long and 12 or 18 mm in diameter. For convenience this material will be referred to as “enriched” HAPEX (E.HAPEX).

The rods of E.HAPEX were powderized as above and blended with the chopped HMPE fibers following a similar technique as used for the HA/chopped fiber system. The proportion of the various materials used were chosen such that the final mix achieved the predetermined HA content, while two-thirds by volume of the PE had fiber morphology.

### Hydrostatic Extrusion (HE)

Details of the experimental procedure may be seen in a previous publication.<sup>9</sup> Thus, only a brief summary is presented.

The apparatus used for HE is shown in Figure 1. The die had a cone semiangle of 15° with bore

diameters of 1.8 mm, 2.5 mm, or 3.5 mm, according to the extrusion ratio (ER = 4 : 1, 7 : 1 or 11 : 1) and the original dimensions of the compacted bars. Billets were machined from the bars into cylindrical rods with a 15° nose to create an initial pressure seal. At the tip of the nose a constant diameter stub was machined, which protruded a few millimeters through the die. A cable attached to the stub was used to drive a rotary potentiometer to provide a displacement signal which was recorded throughout the extrusion stage. A haul-off load of 40–100 g was attached to the free end of the cable to ensure a firm drive of the rotary potentiometer. The back 3 mm of the billet were machined to a larger diameter to act as a plug and prevent the violent release of pressure and hot fluid at the end of the run.

The pressurizing fluid was castor oil (J. L. Seaton, Hull, UK). The billets were coated with two layers of Evostick (Evolve Ltd., Stafford, UK) to avoid direct contact between the polymer matrix and the pressurizing fluid, which involves a risk of stress cracking.<sup>9</sup> Each applied layer of glue was allowed to dry for several hours. It was found that the Evostick coating peeled off during extrusion and did not go through the die.

The extrusion pressure was a function of the material and the extrusion ratio, varying between 10 and 96 MPa. There was little control of the extrusion rate, which was ~ 1.5 mm min<sup>-1</sup>.

### Differential Scanning Calorimetry (DSC)

The effect of the various processing stages (blending, compaction, powderizing, recompaction, and hydrostatic extrusion) on the morphology of the PE matrix was qualitatively assessed by studying the melting behavior of the material. For this purpose, a Perkin–Elmer Differential Scanning Calorimeter DSC7 (Perkin–Elmer

Corp., Norwalk, Connecticut, USA) was used with a scanning rate of  $10^{\circ}\text{C min}^{-1}$  and 2–10 mg of material for each run.

### Optical Microscopy

The effect of the various processing stages on the dispersion of HA in the PE matrix was assessed with optical microscopy. The specimen preparation consisted of sectioning, molding in an epoxy resin, grinding, and polishing, taking particular care in the preservation of the surface structure. For this purpose the critical stage was polishing, carried out for 30 h in a vibratory polisher using Masterprep™ gel polishing suspension (Buehler Krautkramer, Coventry, UK). The prepared samples were examined under a Leitz DMRX microscope (Wetzlar, Germany) using incident light illumination and interference contrast when required.

### Mechanical Testing

Samples were tested in three-point bending. Two types of geometry were used, bars with rectangular cross sections (compacted samples), and cylindrical rods (compacted and hydrostatically extruded samples). Tests of rectangular bars followed ASTM 790<sup>27</sup> recommendations, while rods were tested with their original extruded diameters.

Three main measurements were made in flexure: modulus (FM), strength (FS), and ductility (FD). The formulas used to calculate these properties are given by the simple beam theory.<sup>28</sup> The flexural test parameters and the formulas may be seen in Ladizesky, Ward, and Bonfield.<sup>26</sup> It should be noted here that the flexural modulus was measured with two different gauge lengths, namely 130 mm ( $\text{FM}_{130}$ ) and 50 mm ( $\text{FM}_{50}$ ), while flexural strength and ductility were measured with 50-mm gauge length. The term “ductility” refers to the maximum strain (in %) in the sample at a given deflection. For all samples the following condition applied.

$$\frac{\text{Gauge length}}{\text{Thickness or diameter}} \geq 15$$

Some hydrostatically extruded rods did not break in bending but, instead, the load-deflection graph exhibited a peak stress. In these cases the FS and  $\text{FD}_m$  were measured at maximum stress. A fur-

ther value of the maximum strain in the rod ( $\text{FD}_{-25}$ ) was calculated when the load decreased by 25% after the peak. However,  $\text{FD}_{-25}$  is only quoted for samples which showed no crack formation beforehand, as evidenced by a steplike decrease in the load-deformation graph.

All the mechanical tests were carried out at room temperature ( $22.0 \pm 1.5^{\circ}\text{C}$ ) using an Instron TT-CM (Instron Ltd, High Wycombe, UK). Owing to the large number of systems studied, it was decided to use a minimum of three nominally identical samples for any specific test. However, this number was often increased through the availability of samples made for other experiments. The maximum standard deviations (SD, in percent of the property value) are shown in Table II.

## RESULTS

Prior to the main experiments, which will be presented in detail below, a wide range of preliminary flexural tests were carried out in order to assess the effect of the various variables involved in the preparation and testing of the samples (sample geometry, compaction and recompaction temperatures, powderizing with sieves of different perforation size, temperature during hydrostatic extrusion). The conclusions of these preliminary experiments were used to define the main parameters of the subsequent, more detailed experiments and are presented qualitatively as follows.

### Preliminary Experiments

#### Blending Technique

No significant difference was found in the mechanical properties and HA dispersion in samples made with the room temperature or liquid nitrogen blending techniques. Therefore, this variable is omitted from the remainder of this communication.

#### Sample Geometry

The effect of geometry (rectangular plates or cylindrical rods) was studied with compacted bars containing 30 vol % HA. These were produced with the standard plate geometry (5 samples) and also machined into rods with diameters between 1.8 mm and 4.5 mm (9 samples). No significant

**Table II Maximum (Average) Percent SD for Flexural Tests**

System	Powderizing	Hydrostatic Extrusion <sup>a</sup>	Flexural Properties		
			Modulus	Strength	Ductility
HAPEX™ (40 vol % HA)	N/A	(1)	13 (7)	11 (8)	20 (12)
100% chopped fiber	No	(2)	30 (18)	20 (20)	50 (40)
	Yes	(1)	6 (4)	4 (3)	15 (6)
HA/chopped fiber	No	(2)	20 (10)	14 (9)	50 (32)
	Yes	(1)	11 (4)	15 (5)	40 (10)

<sup>a</sup>(1) Includes samples with and without hydrostatic extrusion. (2) Only samples without hydrostatic extrusion.

differences were found in the mechanical properties calculated with samples of either geometry.

For most systems the modulus was determined at two different gauge lengths, 130 and 50 mm. The larger gauge length gave values up to 15% higher than those obtained with the shorter gauge length. This trend applied to both hydrostatically extruded and to nonextruded samples.

### Compaction Temperature

For 100% compacted HMPE fiber samples, best mechanical properties were obtained at a compaction temperature of 136.5°C. When HA was added, best mechanical properties were obtained with compaction temperatures of 137.5°C for 20 vol % HA and 138.0°C for higher HA content. However, if the filler was incorporated in the form of E.HAPEX, best mechanical properties were obtained when the compaction temperature was reduced by 0.5°C because HAPEX™ contributes a lower melting point PE fraction to the matrix.

Compaction temperatures below those given above resulted in slightly powdery composites with inhomogeneous appearance, while higher compaction temperatures were generally associated with a decrease of stiffness and strength, which became severe at 140°C.

### Powderizing and Recompaction

The recompaction temperature of powderized samples had minimal effect on the mechanical properties provided it remained between 3.0 and 4.0°C below the first compaction temperature. Therefore, this parameter will not be mentioned again in the remainder of this article.

Powderizing had a pronounced effect in both the processability and the mechanical properties of the composites. The main effects may be summarized as follows: (1) Powderizing was associ-

ated with a significant decrease in the scatter of results obtained from nominally identical samples (see Table IV). (2) Powderizing with sieves of 2-mm perforations or smaller significantly decreased the stiffness and strength of the resultant composites. (3) Powderizing and re-compaction are essential stages for successful hydrostatic extrusion. Broadly, the smaller the sieve perforations the more homogeneous and trouble-free the hydrostatic extrusion process. The extruded products of nonpowderized billets and those powderized with sieves of 6-mm perforations showed a number of weak regions where fracture occurred readily, even during the extrusion process. Samples with up to 40 vol % HA powderized with 0.5 mm perforation sieves extruded satisfactorily. Successful extrusion of composites containing 50 vol % HA could only be achieved after powderizing with 80- $\mu$ m perforations sieves. No hydrostatic extrusion experiments were carried out using samples powderized with sieves perforations intermediate between 6 and 0.5 mm.

### Extrusion Temperature

Previous work<sup>9</sup> showed that linear PE should be extruded at 100°C for the best balance between the increasing deformability of the material and loss of product properties due to annealing effects at higher temperatures. Initial experiments showed that the composite systems studied in this research required a higher temperature for successful hydrostatic extrusion, and 115°C was adopted throughout.

Table III summarizes the conclusions of the preliminary experiments and, where applicable, gives the parameters used for the main experiments.

## Main Experiments

### Mechanical Measurements

Tables IV and V give the flexural properties with, for comparison, results obtained with composites

**Table III Conclusions Obtained from the Preliminary Experiments**

Variable	Conclusions (Parameters)
Sample/test geometry	Rectangular plates and cylindrical rods give similar flexural properties. Changing the gauge length from 130 to 50 mm decreases the calculated stiffness by up to 15%.
Blending technique	Similar results were obtained with samples mixed with either the room temperature or the liquid nitrogen technique
Compaction temperature	Optimum (for best mechanical properties) 0 vol % HA, 136.5°C; 20 vol % HA, 137.5°C; >20 vol % HA, 138.0°C The optimum compaction temperature is reduced by 0.5°C when the HA is incorporated in the form of "enriched" HAPEX  Compaction temperatures higher than those given above decrease the stiffness and strength of the material
Powderizing and recompaction	Powderizing decreases the scatter of results obtained from nominally identical samples Powderizing decreases the stiffness and strength Successful hydrostatic extrusion requires a powderizing stage with perforation sieve as follows: up to 40 vol % HA—0.5 mm, 50 vol % HA—80 μm Recompaction has to be carried out at 3.0–4.0°C below the first compaction temperature.
Extrusion temperature	115°C

not involving chopped HMPE fibers. It is seen that all the hydrostatically extruded composites readily achieve the level of stiffness and strength associated with cortical bone, as well as satisfactory ductility. On the other hand, none of the composites without hydrostatic extrusion possess properties comparable to the biological tissue.

When comparing the systems without hydrostatic extrusion, Table IV shows that the properties of HAPEX™ are broadly matched by the properties of HA/chopped HMPE fiber composites. However, after hydrostatic extrusion the properties of HA/chopped HMPE fiber composites are superior to extruded HAPEX™ (Table V).

### Die Swell

Polymeric materials usually swell on leaving the die. This effect is known as "die swell" and Gibson and Ward<sup>9</sup> defined it as

$$\frac{d_e - d_d}{d_d} \times 100 \quad (1)$$

where  $d_e$  and  $d_d$  are the extrudate and die bore diameters, respectively. Equation (1) will be referred to as diametrical die swell. However, when dealing with composite materials it is more useful to define die swell in terms of the cross-sectional areas of the extrudate  $A_e$  and of the die bore  $A_d$ ,<sup>26</sup> namely

$$\frac{A_e - A_d}{A_d} \times 100 = \frac{(d_e)^2 - (d_d)^2}{(d_d)^2} \times 100$$

which will be called cross-sectional die swell. The values of the diametrical and cross-sectional die swells are given in Table V. The standard deviation along an extrudate rod was < 2% in all cases. Table V shows two extrusion ratios, namely the nominal and the actual, calculated with the die bore and extrudate diameters, respectively.

Table V indicates that the cross-sectional die swell is > 10% only for low extrusion ratio (4 : 1) and HA content up to 30 vol %. In all other cases the die swell is relatively small, namely ≤ 6%.

**Table IV Flexural Properties of Nonextruded HA/Chopped HMPE Fiber Composites**

HA Content (vol %)	Powderizing (sieve perforation, mm)	Flexural Properties				
		Modulus (GPa)		FS (MPa)	Ductility (%)	
		FM <sub>130</sub>	FM <sub>50</sub>		FD <sub>m</sub>	FD <sub>-25</sub>
Cortical bone (ref. 19)		7–30		50–150	0.5–3.0	
HAPEX <sup>TM</sup> (40 vol % HA)	—	—	4.7	32	1.4	—
0	—	6.8	4.8	52	2.5	4.8
	0.5	2.7	2.4	34	3.9	7.4
20	—	6.3	5.8	49	2.8	4.3
	0.5	4.0	3.6	41	2.7	7.8
30	—	5.2	5.0	37	2.8	5.1
	0.5	5.8	3.9	42	1.6	—
30*	—	6.3	5.5	47	2.3	—
	0.5	4.9	4.2	38	1.9	—
40	0.08	7.4	6.1	36	0.8	—

## DISCUSSION

### Choice of HA/PE Composite for Bone Substitute Applications

The flexural tests results (Tables IV and V) provide an early indication of the suitability of the various systems studied for load-bearing implants.

Based on the mechanical properties, Table IV indicates that there is no significant difference between HAPEX<sup>TM</sup> and HA/chopped HMPE fiber composites for minor load-bearing applications. However, HAPEX<sup>TM</sup> may be the system of choice because (1) there are extensive previous studies of this system, including its biocompatibility<sup>17–24</sup>; and (2) the hot compounding process used to produce HAPEX<sup>TM</sup> gives homogeneous dispersion of the HA particles in the PE matrix<sup>24</sup> while the room temperature mixing of the two components cannot achieve a similar level of homogeneity, even after powderizing (see below).

Table V shows that, for implants under substantial physiological loads, extruded HA/chopped HMPE fiber composites appear more suitable than extruded HAPEX<sup>TM</sup>, mainly on account of consistently superior stiffness. Systems with the HA incorporated as a powder also show higher strength, while those produced with E.HAPEX have a somewhat reduced strength, broadly similar to the strength of extruded HAPEX<sup>TM</sup>. The decrease in strength is probably associated with a lower fiber morphology fraction in the PE phase. The ductility of the extruded HA/chopped HMPE

fiber systems is generally similar to the upper levels associated with cortical bone, but somewhat lower than the values obtained with extruded HAPEX<sup>TM</sup>.

### Other Aspects of the Mechanical Properties

Powderizing and recompaction affects the relationship between the HA content and the mechanical properties of the unextruded materials. Table IV shows that for bars made without the powderizing stage the flexural properties are broadly independent of the HA fraction. This feature suggests that the reinforcing effects of the fiber morphology and those of the particulate ceramic broadly balance each other. Therefore, as the fiber morphology fraction decreases, the additional filler maintains the level of mechanical performance of the composite.

For powderized and recompacted materials the relationship between HA content and the mechanical properties of the unextruded bars are somewhat more complex. Table IV shows that an increase in the HA fraction is associated with increasing stiffness and decreasing ductility. The latter effect obscures the trend applicable to the flexural strength because a ductile/brittle transition takes place as the HA content increases. Similar effects were observed by Wang, Porter, and Bonfield<sup>24</sup> for the tensile properties of isotropic HA/PA composites. It may be argued that the powderizing process reduces the fiber morphology fraction of the HA/chopped HMPE fiber systems



**Table V Flexural Properties of Hydrostatically Extruded HA/Chopped HMPE Fiber Composites**

HA Content (vol %)	ER		Die Swell (%)		Extrusion Pressure (MPa)	Flexural Properties				
	Nominal	Actual	Diametrical	Cross Section		Modulus (GPa)		FS (MPa)	Ductility (%)	
						FM <sub>130</sub>	FM <sub>50</sub>		FD <sub>m</sub>	FD <sub>-25</sub>
HAPEX <sup>TM</sup> (40 vol % HA)	8 : 1	—	—	—	—	10.1	9.1	91	6.9	15.1
	11 : 1	—	—	—	—	10.8	10.9	79	4.1	8.4
0	4 : 1	3.5 : 1	6	13	10	8.4	6.9	88	6.0	10.7
	7 : 1	6.9 : 1	1	2	17	12.7	12.7	103	3.9	7.6
20	7 : 1	6.9 : 1	1	2	28	17.5	15.2	119	3.6	—
30	4 : 1	3.6 : 1	6	13	29	9.6	9.3	86	3.4	7.3
	7 : 1	6.7 : 1	3	5	45	16.3	15.5	104	3.0	6.9
	11 : 1	10.5 : 1	2	5	58	19.6	19.5	117	2.8	6.5
30 <sup>a</sup>	4 : 1	3.9 : 1	1	2	—	8.9	9.0	75	3.6	7.5
	7 : 1	6.8 : 1	2	3	41	14.2	11.9	87	3.3	—
	11 : 1	10.7 : 1	1	3	59	16.6	15.2	113	2.8	—
40	4 : 1	4.0 : 1	0	0	24	10.5	10.8	86	3.8	8.5
	7 : 1	6.8 : 1	2	3	38	14.4	14.1	97	3.8	—
50 <sup>a</sup>	7 : 1	6.7 : 1	2	4	62	11.9	12.4	72	2.8	5.9
	11 : 1	10.4 : 1	3	6	96	13.6	13.5	69	1.6	—

<sup>a</sup> For these systems the HA was incorporated as “enriched” HAPEX (see text).

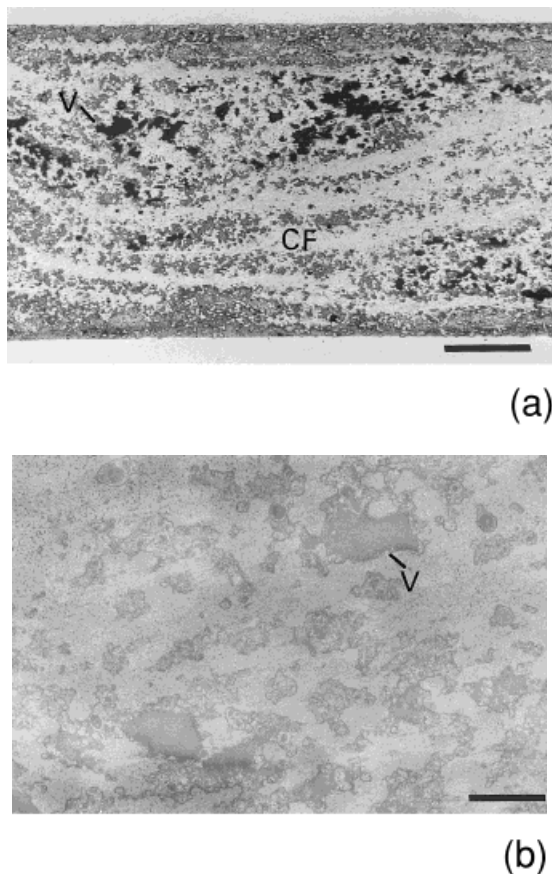


**Figure 2** Polished cross section of nonpowderized HA/chopped HMPE fiber sample compacted at 138.5°C, 30 vol % HA, as supplied. CF, cluster of compacted fibers; V, void. (a) Cursor = 500  $\mu\text{m}$ , (b) cursor = 50  $\mu\text{m}$ .

(see below) and the filler becomes the main reinforcing factor. Indeed, at similar HA content the flexural properties of powderized and recompacted HA/chopped HMPE fiber composites match those of the isotropic HAPEX<sup>TM</sup> (Table IV).

### Optical Microscopy Studies

Figures 2–4 are optical micrographs of polished cross sections of HA/chopped HMPE fiber composite bars containing 30 vol % HA. Figure 2(a,b) correspond to a nonpowderized sample with the HA incorporated as supplied. The HA/PE distribution is inhomogeneous and a number of voids can be seen, suggesting insufficient production of recrystallized polymer during the compaction stage. Figure 3(a,b) are also optical micrographs of a nonpowderized sample, but in this case the HA was incorporated as E.HAPEX. The components are, again, inhomogeneously distributed,

but the voids are completely absent owing to the additional isotropic polymer associated with the powderized composite.

Powderizing and recompaction lead to a dramatic improvement of the homogeneity of the composites. This is seen by comparing Figures 4(a,b) with 2(a,b), respectively, all corresponding to samples with the HA incorporated as supplied. In addition, powderizing and recompaction eliminated the voids.

Figures 2(b) and 3(b) show that nonpowderized samples have well-defined fibers. On the other hand, powderizing and recompaction remove such features [Fig. 4(b)].

The discussion arising from Figures 2–4 can be related to some observations noted in Table III, namely (1) successful hydrostatic extrusion of HA/chopped HMPE fiber composites required

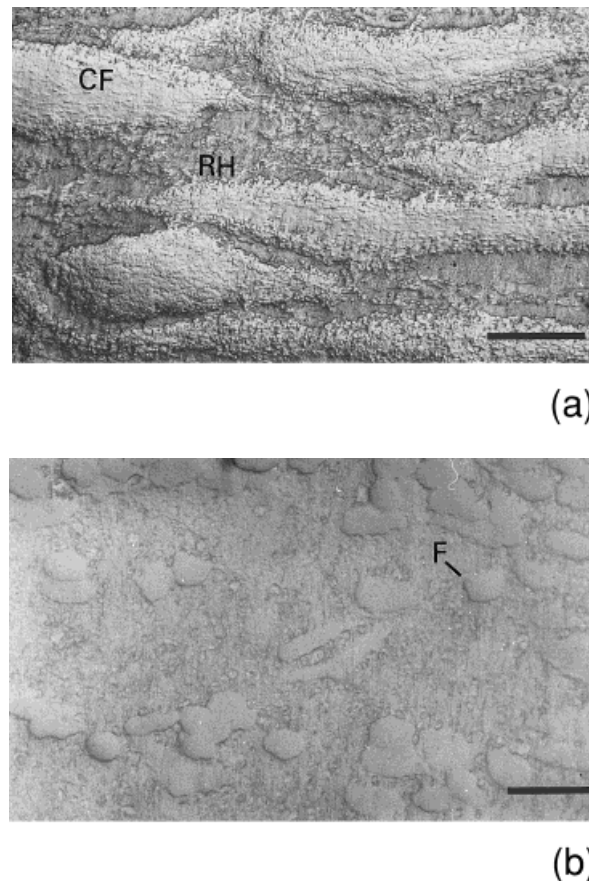
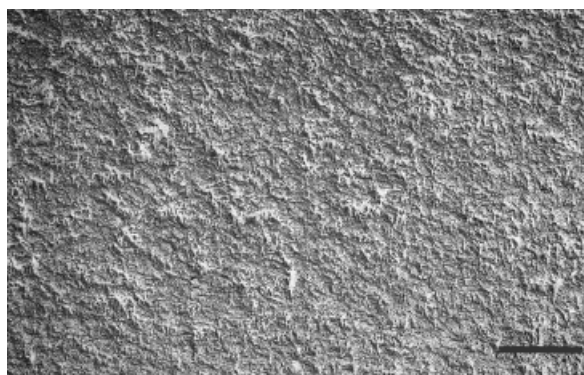
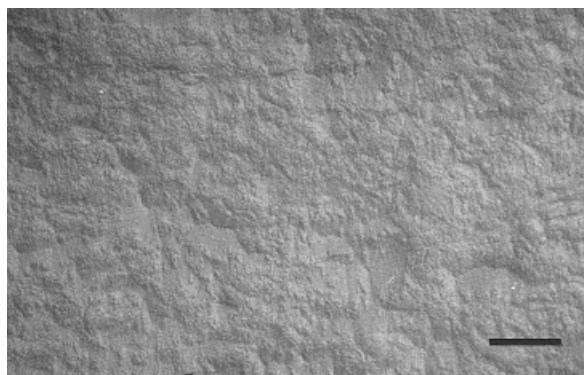


**Figure 3** Polished cross section of nonpowderized HA/chopped HMPE fiber sample compacted at 138.0°C, 30 vol % HA, incorporated as E.HAPEX. CF, cluster of compacted fibers; RH, region rich in HA/recrystallized polymer; F, isolated fiber. (a) Cursor = 500  $\mu\text{m}$ , (b) cursor = 25  $\mu\text{m}$ .



(a)



(b)

**Figure 4** Polished cross section of HA/chopped HMPE fiber sample compacted at 138.0°C, powderized down to 0.5 mm sieve and recompact. 30 vol % HA, as supplied. (a) Cursor = 500  $\mu\text{m}$ , (b) cursor = 100  $\mu\text{m}$ .

a powderizing and recompact stage [compare voids and/or inhomogeneous phases distribution seen in Figs. 2(a) and 3(a) with the homogeneous, void free appearance of Fig. 4(a)]. (2) For nonextruded systems, the flexural test results show that (a) the powderizing and recompact stage enhanced the reproducibility among nominally identical samples [same comparison as (1) above] and (b) powderizing and recompact decreased the stiffness and strength of the composites [loss of fiber structure, as seen by comparing Figs. 2(b) and 3(b) with 4(b)]. The latter finding will be further discussed in the next section.

### DSC Studies

DSC is a useful experimental technique to study the effect of the processing parameters on the morphology of HA/chopped HMPE fiber compos-

ites. Table VI gives a summary of the experimental procedures involved in the production of the samples.

### Procedure Prior to Bar Production

Figure 5(a,b) show DSC scans obtained with virgin continuous HMPE fibers (as supplied in bobbins) and after chopping, respectively. The fibers melt over a narrow range of temperatures at  $\sim 143.0^\circ\text{C}$  and the chopping procedure has no significant effect.

### Procedures During Bar Production

Figure 6(a) shows a DSC scan obtained with a 100% chopped HMPE fiber bar compacted at 136.5°C. It is seen that the compaction has produced a small amount of recrystallized PE (low melting point). This bar has a translucent, homogeneous appearance. Compacting below this temperature results in bars with whitish regions, suggesting incomplete wetting of the fibers by the melted and recrystallized PE. Therefore, a compaction temperature in the region of 136.5°C is considered optimal for the production of 100% chopped HMPE fiber bars (Table III).

Increasing the compaction temperature to 137.5°C still produces homogeneous, translucent bars, but Figure 6(b) shows that the melting peak of the recrystallized PE fraction moves to higher temperatures and, more importantly, the ratio of the recrystallized PE to the PE retaining the fiber morphology increases. This has a deleterious effect on the flexural properties, as noted in Table III.

For composites, a compaction temperature of 136.5°C results in inhomogeneous whitish and

**Table VI** Summary of Experimental Procedures Involved in the Manufacture of HA/Chopped HMPE Fiber Composites

Manufacturing Stage	Procedure
Prior to bar production	Fibre chopping
During bar production	Compaction of fibers
	Without HA
	With HA
	HA as supplied
	HA as "enriched"
	HAPEX <sup>TM</sup>
After bar production	Powderizing
	Recompact
	Hydrostatic extrusion

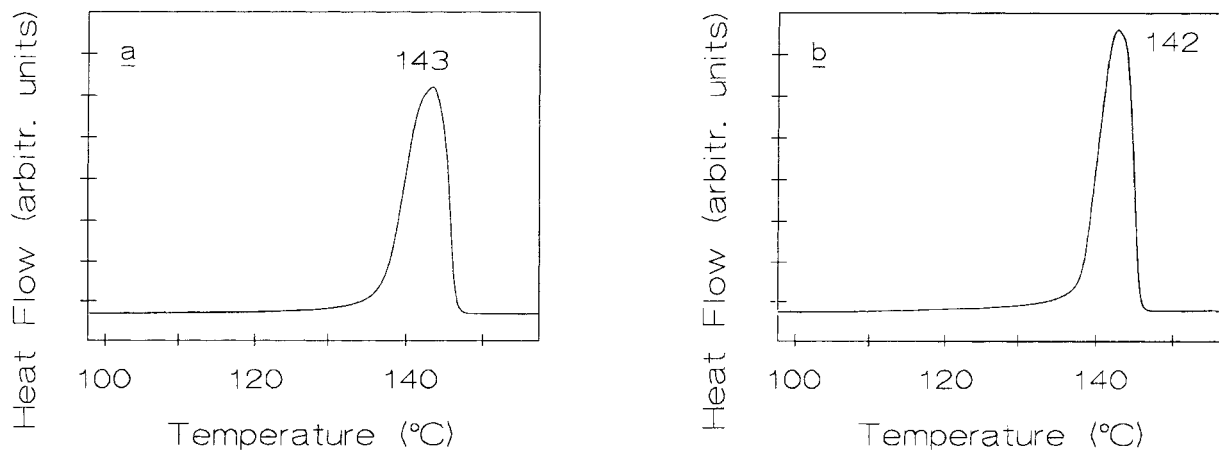


**Figure 5** DSC melting endotherms of HMPE fibers. (a) Continuous thread (from a bobbin), (b) chopped fibers.

powdery bars, with poor mechanical properties. Better appearance and improved properties are achieved at higher compaction temperatures (see Table III). Figure 7(a), when compared with Figure 6(b), shows that the incorporation of 30 vol % HA as a powder does not interfere with the melting behavior of the HMPE fiber during compaction. Furthermore, when the HA is incorporated as E.HAPEX, the melting endotherm of the recrystallized PE fraction has at least two distinct components and, more importantly, this fraction is significantly augmented [Fig. 7(b)]. This explains two previous observations, i.e., that the optimal compaction temperature for composites with a given HA content was reduced by  $\sim 0.5^\circ\text{C}$  by the incorporation of HA in the form of E.HAPEX (Table III); and for hydrostatically extruded samples with 30 vol % HA, Table V shows that

composites with superior mechanical properties are obtained when the HA is incorporated as supplied, rather than in the form of E.HAPEX.

#### Procedures After Bar Production

Figure 8(a–d) shows a sequence of DSC scans obtained with a 30 vol % HA/chopped HMPE fiber composite (HA incorporated as supplied) powdered to 6-mm, 2-mm, 0.5-mm, and 80- $\mu\text{m}$  sieve perforations, respectively. The scans were made with the composite powders; that is, before recompaction. The sequence is completed with Figure 7(a), showing the melting behavior of the compacted system before powderizing. It is seen that powderizing reduces the melting temperature of the fiber morphology fraction while significantly increasing the ratio of the low melting

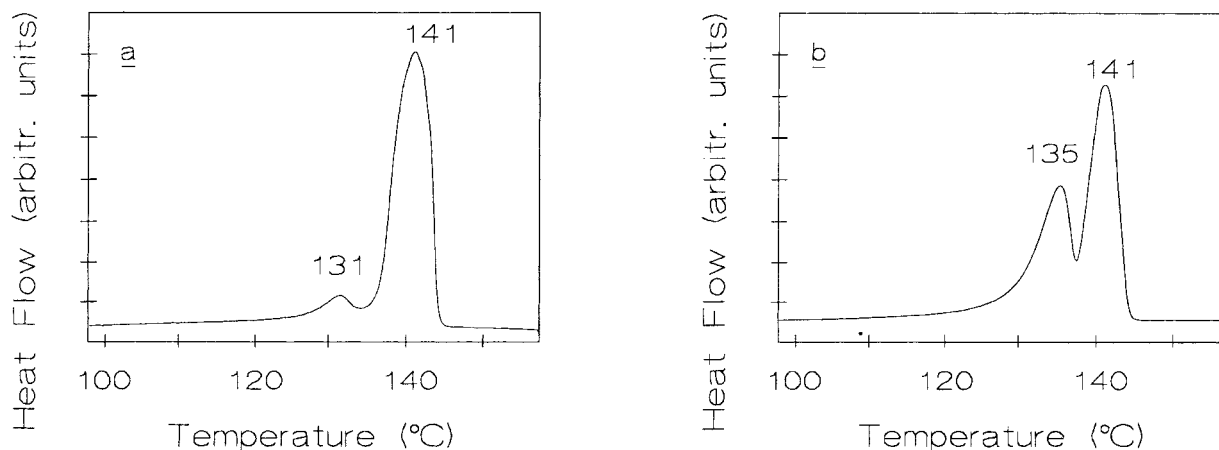


**Figure 6** DSC melting endotherms of 100% chopped HMPE fiber bars compacted at (a)  $136.5^\circ\text{C}$  and (b)  $137.5^\circ\text{C}$ .

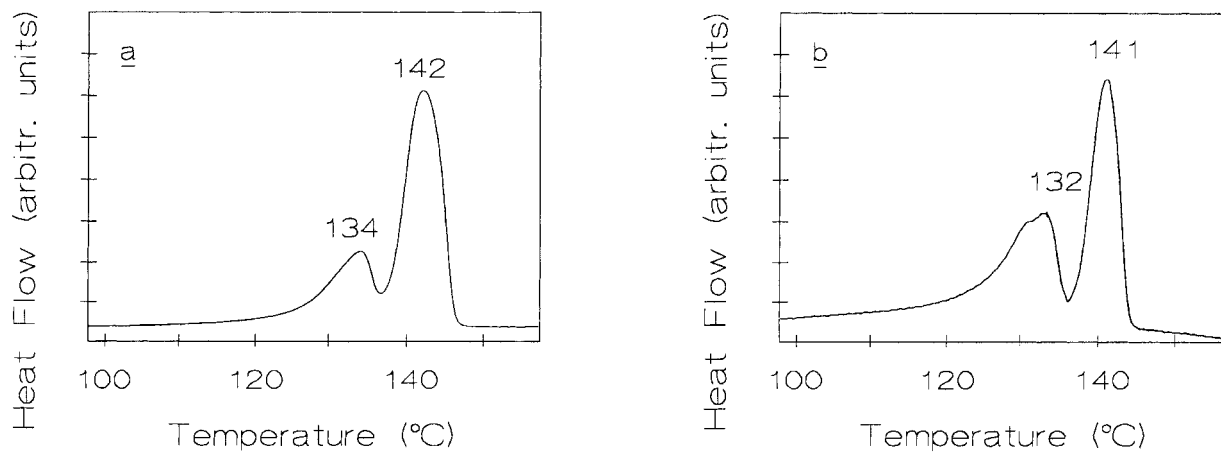


**Figure 7** DSC melting endotherms of HA/chopped HMPE fiber bars. 30 vol % HA, compacted at 138.0°C. (a) HA incorporated as supplied, (b) HA incorporated as “enriched” HAPEX (see text).

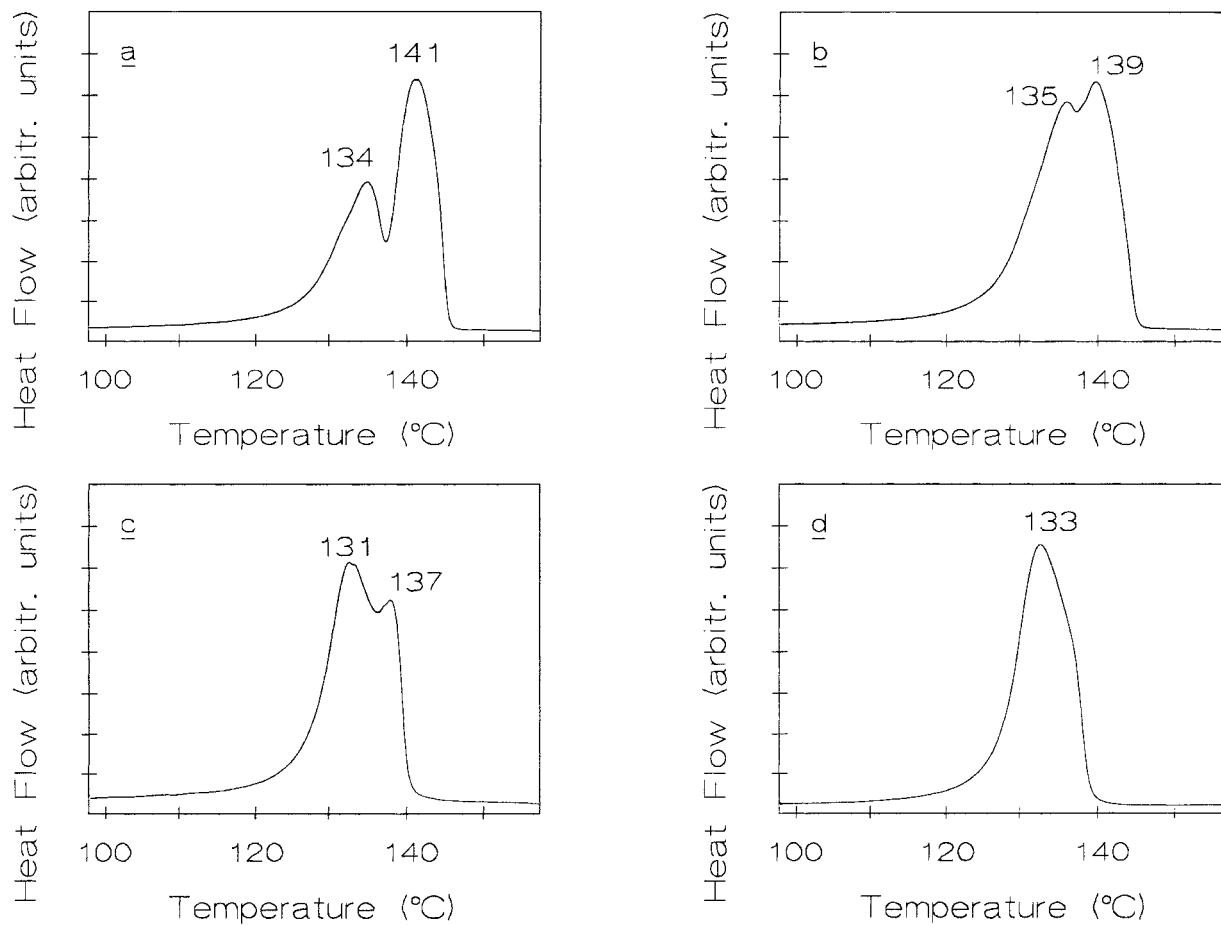


**Figure 8** DSC melting endotherms of HA/chopped HMPE fiber composites. 30 vol % HA, as supplied. Compacted at 138.0°C and powderized using sieves with perforations down to (a) 6 mm, (b) 2 mm, (c) 0.5 mm, (d) 80  $\mu\text{m}$  (samples used in powder form, that is, without recompaction).

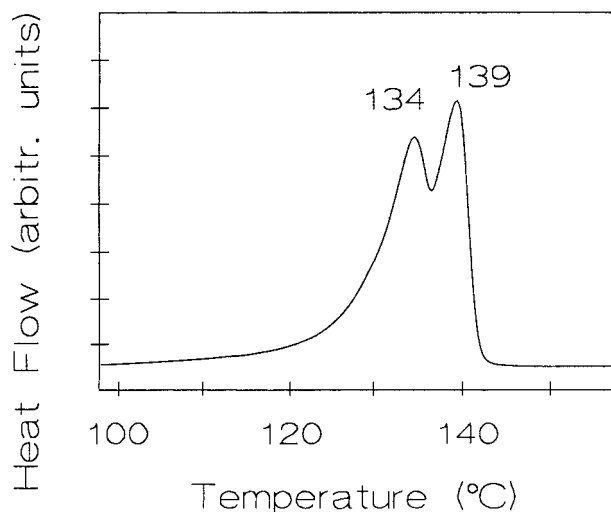


**Figure 9** DSC melting endotherm of HA/chopped HMPE fiber bar. 30 vol % HA, as supplied, compacted at 138.0°C, powderized down to 0.5-mm sieve perforations and recompactd at 134.0°C.

temperature/high melting temperature fractions. A comparison of Figure 9 with Figure 8(c) reveals that recompactd decreases the ratio of the low melting temperature/high melting temperature fractions of the material. It may be argued that the powderizing stage produces significant damage to the fiber morphology of the PE matrix, increasing the fraction which melts at the lower temperature [Figs. 7(a) and 8(c)]. Recompactd removes some of the structural flaws, and this is accompanied by a reversal of the previous trend, that is, the high melting temperature fraction increases (Fig. 9). However, recompactd of the powderized material does not lead to the full recovery of the fiber morphology, as it may be seen by comparing Figure 9 with Figure 7(a). A similar conclusion was arrived at when discussing the optical microscopy evidence, namely, well-defined fibers in nonpowderized samples (Figs. 2 and 3) compared with the absence of such features in powderized and recompactd composites [Fig. 4(a,b)]. This explains the generally superior mechanical properties displayed by the nonpowderized composites (Table 6a), notwithstanding the higher scatter of these results (Tables II and III).

The effect of hydrostatic extrusion on the matrix morphology of HA/chopped HMPE fiber composites may be seen in Figure 10(a–c) together with Figure 9. Hydrostatic extrusion results in a dramatic recovery of the high melting point structure over and above that taking place during re-

compactd. These changes are enhanced as the extrusion ratio increases, correlating with the higher stiffness and strength of the extruded bars, as shown in Table V. The high melting point structure appearing after hydrostatic extrusion [Fig. 10(a–c)] may correspond to the original fiber morphology, plus a contribution from the orientation of the melted and recrystallized fraction. However, further studies are required to understand the interaction between hydrostatic extrusion of compactd composites containing HMPE fibers and the morphology of the resultant extrudates.

Hydrostatic extrusion was also applied to HAPEX™ with considerable success.<sup>26</sup> The process gave rise to an increase of the melting point of the PE phase [Fig. 11(a,b)], but the peak remained at a significantly lower temperature than that obtained with extruded HA/chopped HMPE fiber composites [Figs. 10(b) and 11(b)]. Thus, the fiber morphology initially incorporated into the HA/chopped HMPE fiber composites appears to contribute to the high melting point of the extruded system, even if significant morphological damage has taken place during the intermediate stages. Also, the difference between the melting points of the polymer phases of the two extruded systems correlates with their respective mechanical properties, namely, the stiffness of extruded HA/chopped HMPE fiber composites is substantially higher than that obtained with extruded HAPEX™ (Table V).

#### Characteristics of the Hydrostatic Extrusion of HA/Chopped HMPE Fiber Composites

Qualitatively, the hydrostatic extrusion characteristics found in the present work match the findings of Gibson and Ward.<sup>9</sup>

#### 100% Chopped HMPE Fiber Extrudates

Table V shows that, for 100% chopped HMPE fiber products, the die swell decreases with increasing extrusion ratios. The agreement with the results obtained by Gibson and Ward<sup>9</sup> is at a quantitative level. Table V also shows that the modulus increases for higher extrusion ratios, as was also the case in the work reported by Gibson and Ward.<sup>9</sup> However, the agreement here is not quantitative because Gibson and Ward<sup>9</sup> reported a value of ~ 7 GPa for ER = 7 : 1, whereas significantly higher values are seen in Table V. This difference may be explained on the grounds that the PE used

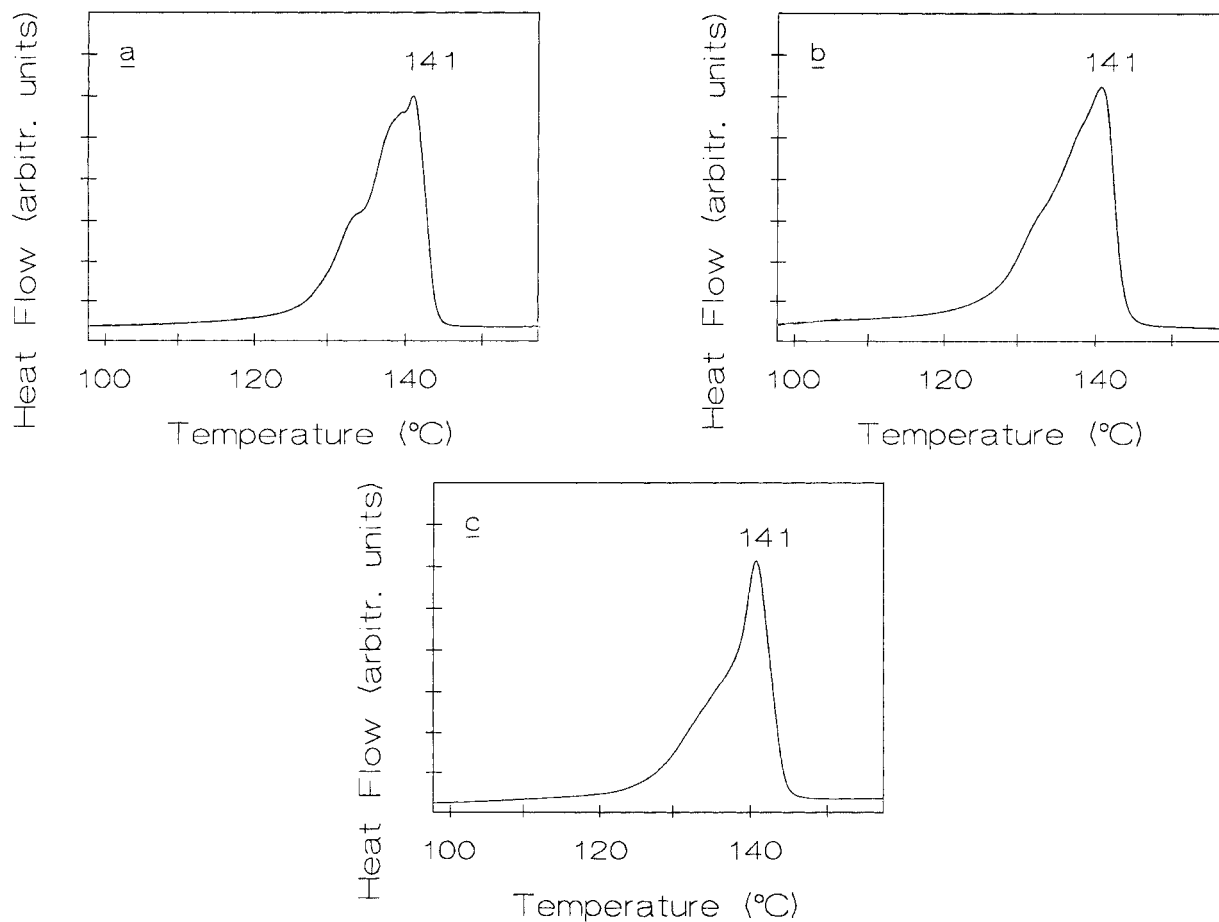


**Figure 10** DSC melting endotherm of HA/chopped HMPE fiber rods. 30 vol % HA, as supplied. Compacted at 138.0°C, powderized down to 0.5-mm sieve perforations, recompactd at 133.0°C–134.0°C, and hydrostatically extruded to (a) ER = 4 : 1, (b) ER = 7 : 1, and (c) ER = 11 : 1.

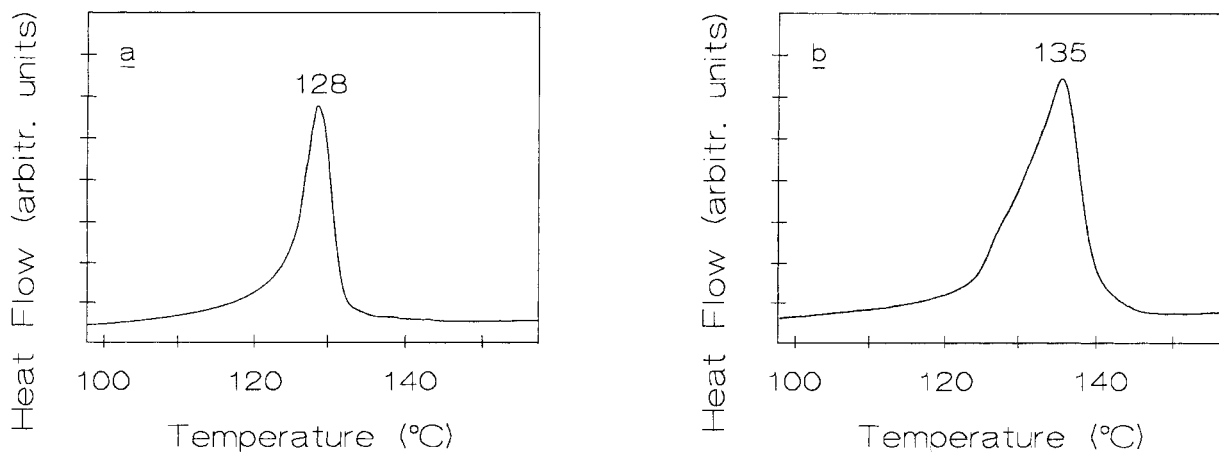


**Figure 11** DSC melting endotherms of HAPEX™ (40 vol % HA). (a) Rod compression molded at 200.0°C, (b) as (a) above, but hydrostatically extruded to ER = 8 : 1.

in the present work has a fiber crystalline morphology, even if this has been affected by the powderizing stage. The fiber morphology is an added element increasing the modulus of the system, on top of the increase induced by the hydrostatic extrusion process.

### HA/Chopped HMPE Fiber Composites

The benefit of fiber morphology on the modulus of the extrudate is maintained for the composite systems. However, the very high modulus attained may have contributions from other mechanisms, such as the reinforcing effect of the filler and, perhaps more importantly, the possibility of an increased orientation of the polymeric matrix because this is the only phase undergoing deformation during the hydrostatic extrusion of composites. Thus, at a given extrusion ratio, the presence of the HA may shift the deformation versus stiffness relationship from the moderate to the steeper rising regime described by Gibson and Ward.<sup>9</sup>

It is instructive to compare the die swell of composites with and without fiber morphology. Figure 12 shows the cross-sectional die swell versus HA content for ER = 7 : 1 of HA/chopped HMPE fiber composites and ER = 8 : 1 of HA/PE systems (PE

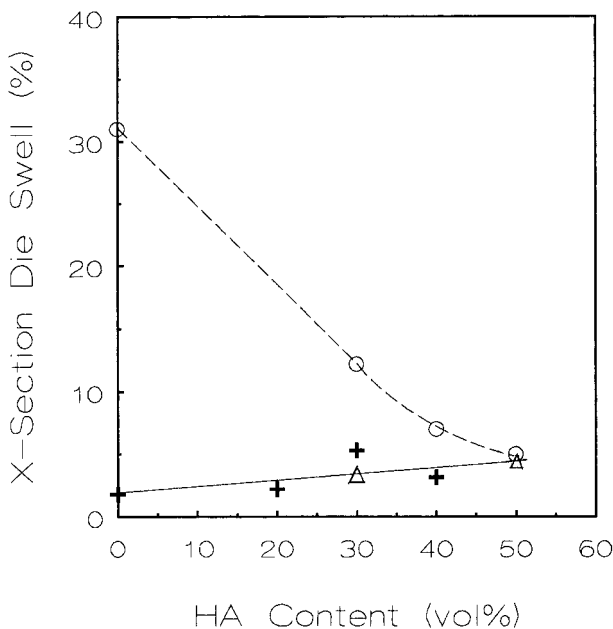


**Figure 12** Cross-sectional die swell versus HA content for (—○—) HA/PE composites (PE = Rigidex HM 4560XP), ER = 8 : 1; and (—) HA/chopped HMPE fiber, ER = 7 : 1 [(+) HA incorporated as a powder; (Δ) HA incorporated as E.HAPEX].

= Rigidex HM 4560XP).<sup>26</sup> For the latter materials, the die swell decreases from a high value of > 30% for 100% PE down to ~ 5% for 50% HA content. This behavior has been explained by Ladizesky, Ward, and Bonfield<sup>26</sup> in terms of results reported by Gibson and Ward<sup>9</sup> plus the possibility of increased deformation of the PE phase induced by the incorporation of HA. On the other hand, the die swell of extruded HA/chopped HMPE fiber composites remains approximately constant below 6% throughout the range of HA content. These widely divergent behaviors may be attributed to the increased geometrical stability of the HA/chopped HMPE fiber system imparted by the fiber morphology of the matrix. Nevertheless, both curves in Figure 12 converge for high HA fractions, suggesting that an increase in HA content is associated with higher orientation in the matrix of the extrudate until this process becomes the dominant factor affecting die swell.

### Extrusion Rate

The mechanisms advanced above also explain the observed narrow extrusion rate range for the systems containing chopped HMPE fiber (see the Experimental section). For a given extrusion ratio, the incorporation of HA may increase the deformation of the matrix, while the fiber morphology contributes with further oriented units, even if their direction is isotropically distributed after powderizing and recompaction. Thus, the narrow range of extrusion rates found for high extrusion ratios ( $E \geq 20 : 1$ ) of isotropic PE<sup>9</sup> is also a feature of the extrusion of HA/chopped HMPE composites for  $ER \leq 11 : 1$ .

### Extrudate Defects

Gibson and Ward<sup>9</sup> reported several types of defects affecting the hydrostatic extrusion of isotropic PE. Some of these defects have also been observed during the hydrostatic extrusion of isotropic HA/PE composites, but they were not present when using the HA/chopped HMPE fiber systems. In these cases the extrusion was either successful, producing good quality extrudates, or unsuccessful, in which case the extrudates broke during extrusion. This occurred when the billets were not powderized with sieves of sufficiently fine perforations (leading to inhomogeneous HA dispersion) and/or when too much HA was incorporated into the systems for the extrusion ratio attempted.



## Summary of the Discussion

The main aspects of the above discussion of DSC studies and hydrostatic extrusion characteristics of HA/PE composites may be summarized by conveniently assuming that the material behavior is governed by four main parameters: (1) powderizing plus recompaction, (2) hydrostatic extrusion, (3) HA content, and (4) the matrix morphology of the billet (isotropic or fiber structure). These parameters control four main variables: (1) melting temperature, (2) mechanical performance, (3) die swell, and (4) extrusion rate.

Powderizing plus recompaction operations damage the fiber morphology of HA/chopped HMPE fiber composites and lowering the melting temperature of the matrix and causing the mechanical properties of the composites to deteriorate. Hydrostatic extrusion induces orientation in the polymeric phase and (1) increases the melting temperature of the matrix, (2) improves the mechanical performance of the composites. With increasing extrusion ratio, hydrostatic extrusion, (3) lowers the die swell and (4) the composites have a limiting extrusion rate. Incorporation of HA may increase the orientation of the PE matrix during hydrostatic extrusion and (1) lead to further improvements of the mechanical performance of the extrudate, (2) sharply decrease the die swell, and (3) give rise to a limiting extrusion rate for all extrusion ratios covered in this work. Fiber morphology provides a stable crystalline structure resulting in (1) the best mechanical performance after hydrostatic extrusion, and (2) small die swell at all HA content.

## CONCLUSIONS

Hydrostatic extrusion of HA/chopped HMPE fiber composites which have been powderized and recompacted produces materials with the highest stiffness and strength yet encountered with HA/PE bone substitute materials, fully comparable to the values associated with cortical bone. This material therefore shows considerable promise for use in skeletal load-bearing prostheses.

It has been shown that the fiber morphology of the matrix has a positive contribution to the mechanical properties and processing stability of the composites.

We are grateful to D. B. Appleyard and D. Stephenson for their invaluable support in all the technical aspects of this research, also to D. Morgan for sharing his experience with the hydrostatic extrusion technology, all of the IRC in Polymer Science and Technology. Dr. K. E. Tanner and Dr. Min Wang, of the IRC in Biomedical Materials, were always available for helpful discussions, and the latter supplied the HAPEX™ material. M. D. Kateb, of the Faculté des Sciences de l'Université Aix-Marseille II, France, suggested the use of liquid nitrogen for the incorporation of hydroxyapatite particles into an array of HMPE fibers. B. Bousfield and his colleagues at Buehler Krautkramer gave valuable assistance and advice to determine a suitable polishing procedure for the composites. The support of the UK EPSRC for the programmes of both the IRCs is gratefully acknowledged.

## REFERENCES

1. I. M. Ward, *Mechanical Properties of Solid Polymers*, Wiley, Chichester, 1983, Chap. 10.
2. I. M. Ward, *Adv. Polym. Sci.*, **70**, 1 (1985).
3. G. Capaccio and I. M. Ward, *Nature Phys. Sci.*, **243**, 143 (1973).
4. P. Smith and P. J. Lemstra, *J. Mater. Sci.*, **15**, 505 (1980).
5. G. Capaccio and I. M. Ward, *Polymer*, **15**, 233 (1974).
6. G. Capaccio, T. A. Crompton, and I. M. Ward, *J. Polym. Sci.-Polym. Phys. Ed.*, **14**, 1641 (1976).
7. P. D. Coates and I. M. Ward, *Polymer*, **20**, 1533 (1979).
8. A. G. Gibson, I. M. Ward, B. N. Cole, and B. Parsons, *J. Mater. Sci. Lett.*, **9**, 1193 (1974).
9. A. G. Gibson and I. M. Ward, *J. Polym. Sci.-Polym. Phys. Ed.*, **16**, 2015 (1978).
10. P. S. Hope, A. G. Gibson, and I. M. Ward, *J. Polym. Sci.-Polym. Phys. Ed.*, **18**, 1213 (1980).
11. P. S. Hope and I. M. Ward, *J. Mater. Sci.*, **16**, 1511 (1981).
12. I. M. Ward, B. Parsons, and J. F. B. Sahari, U.S. Pat. 4,938,913 (1990).
13. G. Capaccio, I. M. Ward, and F. S. Smith, Brit. Pat. Appl. 9797/74 (1974).
14. P. J. Hine, I. M. Ward, R. H. Olley, and D. C. Bassett, *J. Mater. Sci.*, **28**, 316 (1993).
15. I. M. Ward, P. J. Hine, and K. Norris, Brit. Pat. GB 2,253,420 (1992).
16. R. H. Olley, D. C. Bassett, P. J. Hine, and I. M. Ward, *J. Mater. Sci.*, **28**, 1107 (1993).
17. W. Bonfield, in *Engineering Applications of New Composites*, S. A. Paipetis and G. C. Papanicolaou, Eds., Omega Scientific, Oxford, GB 1988, Chap. 1.
18. W. Bonfield, *J. Biomed. Eng.*, **10**, 552 (1988).
19. J. C. Behiri and W. Bonfield, *Biomedizinische Technik*, **33**, 109 (1988).

20. W. Bonfield, J. A. Bowman, and M. D. Gryn timer, Brit. Pat. GB 2,085,461 B, (1984).
21. W. Bonfield, C. Doyle, and K. E. Tanner, in *Biological and Biomechanical Performance of Biomaterials*, P. Christel, A. Meunier, and A. J. C. Lee, Eds., (Proceedings of the fifth European conference on biomaterials, Paris, September 4–6, 1985), Elsevier Science.
22. W. Bonfield, M. D. Gryn timer, A. E. Tully, J. Bowman, and J. Abram, *Biomaterials*, **2**, 185 (1981).
23. W. Bonfield, in *Advanced Series in Ceramics, An Introduction to Bioceramics*, Vol. 1. L. Littench and J. Wilson, Eds., World Scientific Publishing Co., Singapore, 1993, Chap. 16.
24. M. Wang, D. Porter, and W. Bonfield, *Brit. Ceram. Trans.*, **93**, 91 (1994).
25. K. E. Tanner, R. N. Downes, and W. Bonfield, *Brit. Ceram. Trans.*, **93**, 104 (1994).
26. N. H. Ladizesky, I. M. Ward, and W. Bonfield, *Polym. Adv. Technol.* (to appear).
27. ASTM D790M-93 American Society for Testing and Materials, Easton, Maryland (1993).
28. J. G. Williams, *Stress Analysis of Polymers*, Ellis Horwood Ltd, Chichester, 1980.